AIAA 2001-0352
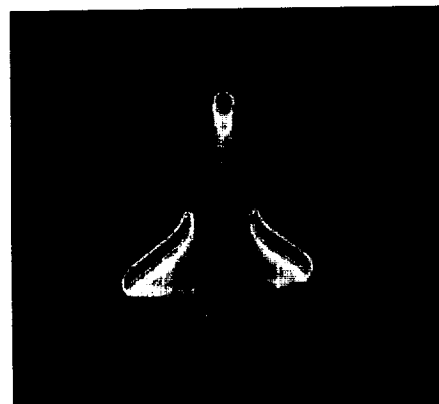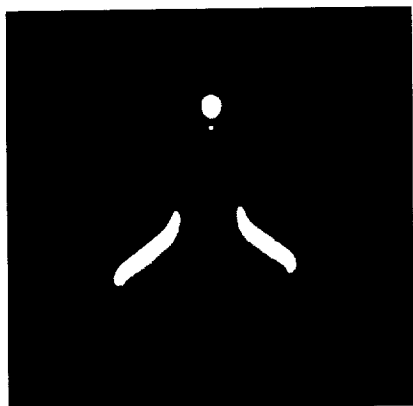
Infrared Sensing Aeroheating Flight Experiment: STS-96 Flight Results

Robert C. Blanchard, Richard G. Wilmoth, Christopher E. Glass
N. Ronald Merski, Jr., Scott A. Berry, Timothy J. Bozung

NASA Langley Research Center,
Hampton, VA 23681-2199

Alan Tietjen, Jodean Wendt, Don Dawson

Computer Sciences Corporation BMDO/Innovative
Sciences and Technology Experimentation Facility
NASA Kennedy Space Center, FL 32899-0001

39th AIAA Aerospace Sciences Meeting & Exhibit
8-11 January 2001 / Reno, NV

Infrared Sensing Aeroheating Flight Experiment: STS-96 Flight Results

Robert C. Blanchard*[†††]
Richard G. Wilmoth*[††]
Christopher E. Glass*[††]
N. Ronald Merski, Jr*[†††]
Scott A. Berry*
Timothy J. Bozung**[†]
NASA Langley Research Center, Hampton, VA 23681-2199

Alan Tietjen[‡‡‡†]
Jodean Wendt[‡‡]
Don Dawson[‡]
Computer Sciences Corporation
BMDO/Innovative Sciences and Technology Experimentation Facility
Kennedy Space Center, FL 32899-0001

Abstract

Major elements of an experiment called the Infrared Sensing Aeroheating Flight Experiment are discussed. The primary experiment goal is to provide reentry global temperature images from infrared measurements to define the characteristics of hypersonic boundary-layer transition during flight. Specifically, the experiment is to identify, monitor, and quantify hypersonic boundary layer windward surface transition of the X-33 vehicle during flight. In addition, the flight data will serve as a calibration and validation of current boundary layer transition prediction techniques, provide benchmark laminar, transitional, and fully turbulent global aeroheating data in order to validate existing wind tunnel and computational results, and to advance aeroheating technology. Shuttle Orbiter data from STS-96 used to validate the data acquisition and data reduction to global temperatures, in order to mitigate the experiment risks prior to the maiden flight of the X-33, is discussed. STS-96 reentry midwave (3-5 μm) infrared data were collected at the Ballistic Missile Defense Organization/Innovative Sciences and Technology Experimentation Facility site at NASA-Kennedy Space Center and subsequently mapped into global temperature contours using ground calibrations only. A series of image mapping techniques have been developed in order to compare each frame of infrared data with thermocouple data collected during the flight. Comparisons of the ground calibrated global temperature images with the corresponding thermocouple data are discussed. The differences are shown to be generally less than about 5%, which is comparable to the expected accuracy of both types of aeroheating measurements.

Nomenclature

c   = speed of light
B_{set} = calibration offset values obtained during system setup
G_{set} = calibration gain values obtained during system setup
h   = Planck's constant
k   = Boltzman's constant
$L_{BB}(T)$ = surface squareband blackbody radiance
L_m = blackbody spectral radiance

L_p = apparent radiance at focal plane
L_{path} = atmosphere band radiance
R   = detector response (counts)
T   = surface temperature (K)
$\epsilon(T)$ = surface emissivity
λ = wavelength
τ_{atm} = path transmittance

Introduction

Atmospheric reentry boundary layer transition, corresponding to a sudden increased surface heating associated with the vehicle boundary layer going from laminar to turbulent flow, has been demonstrated in both flight data and wind tunnel testing. This heating phenomenon impacts thermal protection system (TPS) material selection, split-line location, and material thickness which results in a prominent weight impact and presents challenges for future Reusable Launch Vehi-

---

*Aerospace Technologist, Aerothermodynamics Branch
**Graduate Research Scholar Assistant, George Washington University
[†]Research Scientist
[††]Engineer
[†††]Senior Research Scientist
[†]Member; [††] Senior Member; [†††] Associate Fellow, AIAA

cles (RLV's). The increased heating to the vehicle surface is significant when this transition occurs as increases of a factor of two, or more, in heating level occur on the windward surface of the vehicle. Boundary layer transition occurs "naturally" as a reentry vehicle descends to higher densities, corresponding to increased Reynolds number, and its occurrence has been well demonstrated with "smooth" models in wind tunnels for many years.[1] As observed for the Shuttle Orbiter, transition can occur early in the entry trajectory due to "roughness" factors.[2] Thus, one design goal for the TPS is to constrain the vehicle surface roughness in an attempt to avoid early transition. Also, there are typically flight operation impacts such as, flight-to-flight inspections and maintenance to reduce the risk of early transition. Progression to a full RLV requires that the boundary layer transition effects be well understood and taken into account in any RLV design.

Correlation parameters have been formulated to approximate conditions at which boundary layer transition will occur in flight. For example, the incipient, critical, and effective roughness Reynolds numbers have been used in the heating analysis of the first flights of the Shuttle Orbiter[3]. The correlation parameters are semi-empirical in so far as transition criteria are dependent upon design factors that are developed through wind tunnel or flight experiments, or a combination of both. Also there is the micro- and macro-surface dependency, i.e. forward surface protuberances can trigger early transition, while other material surface properties need to be taken into account for the actual flight vehicle, particularly surfaces that are sensitive to thermal expansion.

The correlation factor used to estimate flight boundary layer transition for the X-33 is Re_θ (momentum thickness Reynolds number) divided by M_e (boundary layer edge Mach number).[4] This correlation factor for the X-33 metallic TPS has been developed in a synergistic approach between computational fluid dynamics (CFD) and wind tunnel tests. It is important to verify this correlation with the flight vehicle, and although the X-33 is equipped with arrays of surface thermocouples, global information is required for a definitive observation of the complex boundary layer transition. Accordingly, an infrared imaging experiment has been devised to provide global temperature images to define the character of the transition period during flight. The experiment is called the Infrared Sensing Aeroheating Flight Experiment (ISAFE) and is discussed in this report (some experiment details also found in the proposal, NRA 8-21, "Flight Technologies for Reusable Launch Vehicles", Langley Research Center, dated April 3, 1998). In addition, the ISAFE methodology is being developed as a general versatile tool to provide flight global heating data for reentry vehicles at hypervelocity speeds.

Four main areas of work are required for the successful accomplishment of ISAFE. These areas are: (1) site selection; i.e. where to put the portable optical mounts; (2) data acquisition; i.e. target acquisition, tracking, and data recording; (3) data reduction to global temperature time histories; and (4) comparison of the flight results to theory, wind tunnel data, and/or CFD simulations. The Shuttle Orbiter was chosen as a flight target to minimize the experiment risks of acquiring useful flight data prior to the maiden flight of the X-33. The Orbiter has many of the elements needed to check out the software and data reduction techniques required to produce global surface temperatures, including onboard surface thermocouples. For the initial ISAFE checkout, it was decided to concentrate on areas (2) and (3) by keeping the optical mounts at the Ballistic Missile Defense Organization/Innovative Sciences and Technology Experimentation Facility (BMDO/ISTEF) site at NASA-Kennedy Space Center (KSC). This report presents a discussion of the ISAFE and presents the data acquired, as well as the analysis of the flight data on the STS-96 Orbiter reentry.

Experiment Objectives

The objective of the Infrared Sensing Aeroheating Flight Experiment is to identify, monitor, and quantify hypersonic boundary layer transition for the X-33 vehicle during flight. This includes, specifically, the global mapping of the transition movement over the windward surface. The data collected during flight will serve as a calibration and validation of current boundary layer transition prediction techniques. In addition, the flight experiment goal is to provide benchmark laminar, transitional, and fully turbulent global aeroheating data in order to validate existing wind tunnel[5] and computational results,[6] and to advance aeroheating technology.

Experiment Approach

Trajectory Considerations

The experiment technical approach is to collect global windward surface temperature data with ground-based infrared emission cameras as the X-33 descends through the upper atmosphere. The primary emphasis will be to view the X-33 during both the peak heating portion of the trajectory and the region of expected boundary layer transition. Figure 1 is a time history graph of several trajectory parameters, namely, Mach number, altitude (Kft) and angle-of-attack (degs.), for a typical X-33 trajectory emanating from Edwards AFB, CA and landing at Michael AFB, Utah. The approximate regions where boundary layer transition is expected, during both ascent and descent based upon the correlation factor previously discussed, are shown to occur between Mach numbers 8 and 10, corresponding to an altitude between 150 and 180 Kft. These distances are the minimum viewing requirement for a ground-based camera. However, since the angle-of-attack is high in the region of expected transition, optimum viewing of the windward surface may be obtained by placing the mobile mounts forward of the trajectory ground

track even though the slant range is larger than the minimum distance. Coverage of the X-33 surface requires a combined telescope and infrared detector system having adequate resolution for these distances.
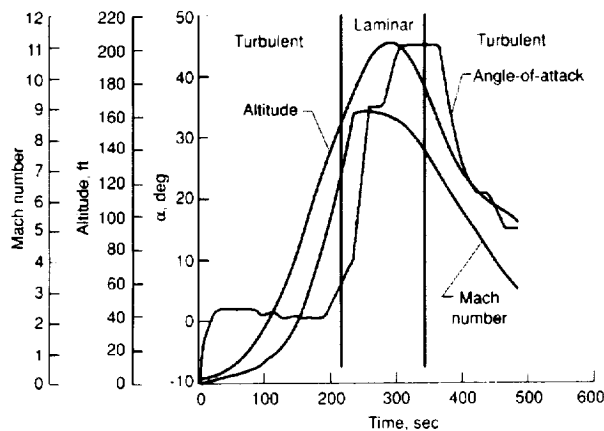

Fig. 1 Typical X-33 trajectory parameters for a Michael AFB landing.

Portable Optical Systems

The measurements will be accomplished nonintrusively (no impact on vehicle airframe, or operations) using ground-based optical instruments of BMDO/ISTEF. The equipment consists of portable optical tracking mounts, which can be equipped with a variety of telescopes (up to 30" apertures), and a variety of detectors ranging in wavelength from ultra-violet to the mid-band infrared, which includes the visible. Figure 2 shows a typical telescope configuration for one of the several tracking mounts in operation at the BMDO facility.
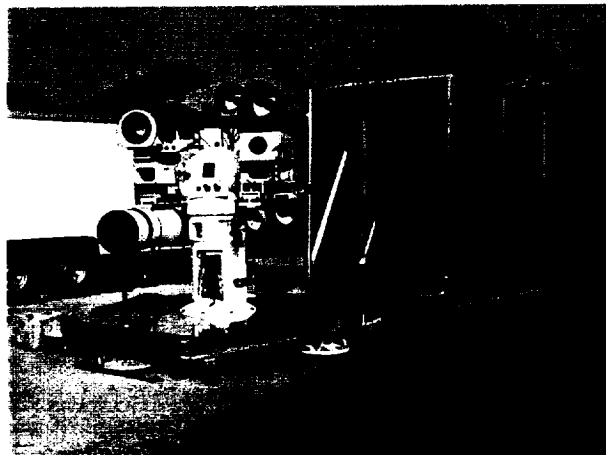
Small Transportable ISTEF Pedestal System (STRIPS) Mount

Fig. 2 Typical BMDO/ISTEF Mobile Optical Tracking Mount.

The 24" telescope shown on the lower left of the mount can be instrumented with a mid-wave infrared

detector to conduct this experiment. The other telescopes can be fitted with other wavelength sensitive detectors (e.g. long wave infrared) so that simultaneous multiple wavelength data can be collected. This has certain advantages to minimizing the atmospheric effects. The mount control system, communications equipment, and data acquisition systems are contained in a mobile trailer (in background) which completes the data collection and tracking system. Extensive software and communication links have been developed for optimally acquiring, tracking, collecting, and reducing flight data.

Tracking Mount Positioning

The optical tracking mount(s) will be strategically positioned very nearly under the planned ground track of the X-33 in order to capture the aeroheating data during flight. Figure 3 shows a typical X-33 ground track for a landing at Michael AFB (corresponding to the trajectory parameters on Fig. 1). For illustration purposes the tracking mobile system is assumed to be directly under the ground track where the X-33 achieves maximum altitude.
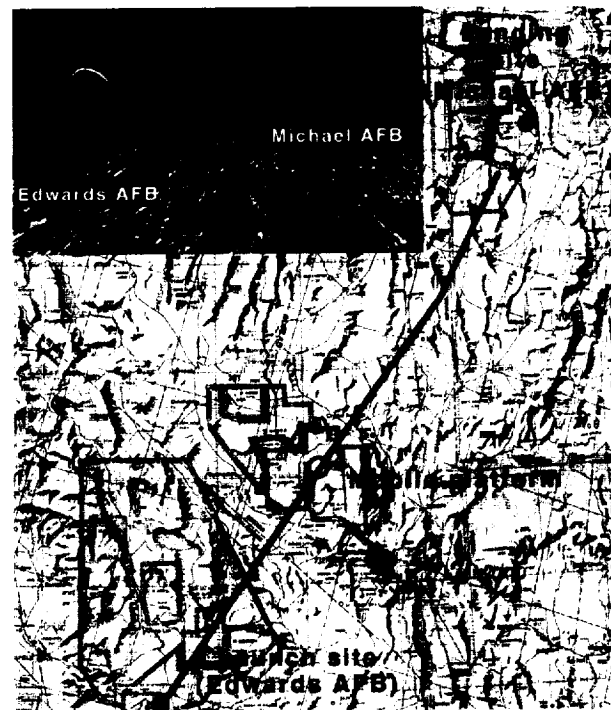

Fig. 3 Typical X-33 ground track from Edwards AFB to Michael AFB.

Simulated optical data were generated to provide thermal map sequences for this trajectory to determine experiment feasibility for the highest altitude. Using the telescope properties and the resolution of the sensor CCD (512x512 pixs.) provided some assurance that a global thermal image is within the capability of the

3

BMDO/ISTEF portable imaging systems. Figure 4 shows a time history of altitude (Kft) and the corresponding approximate image pixel resolution for the simulation. In the region of peak altitude the resolution is about 12 inches for a 60* ft vehicle. This resolution corresponds to about 3 pixels to every two TPS tiles, on the average, roughly equivalent to three thermocouples per two tiles, which should be sufficient to characterize peak heating behavior. For this particular simulation, the resolution is about 30 inches during boundary layer transition, which provides less than optimal coverage. But through optimization of the optical mount location, or application of multiple mounts, resolution during transition can be significantly improved. Other factors, such as atmospheric effects, will need to be taken into account in selecting the final mount location(s).

Infrared radiance images are collected at 30 frames/sec and will be reduced to surface temperature using calibration factors discussed subsequently. Infrared radiance data is recorded typically as 12 bit digital data and analog RS-170 video output. Discrete onboard surface temperature measurements will be compared with calibrated ground-based infrared measurements in order to enhance credibility of quantitative temperature values. Also, post-flight assessments will be performed using wind tunnel data and CFD codes.
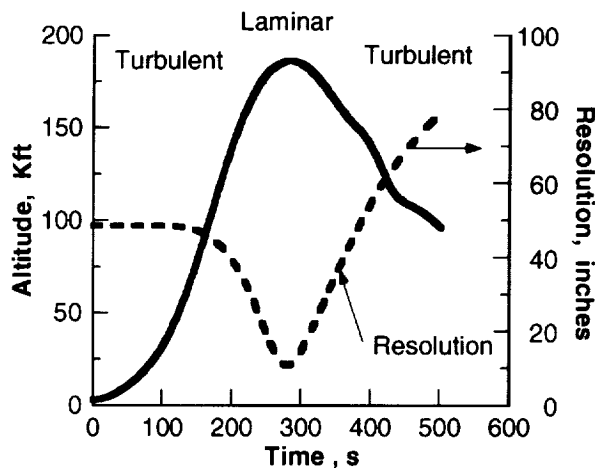

Fig. 4 Altitude and approximate resolution of simulated X-33 images

Shuttle Flight Data

Shuttle Orbiter flights were selected as targets of opportunity to demonstrate the capability of the ground-based infrared equipment and the data reduction techniques, in order to mitigate the aeroheating experiment risks prior to the maiden flight of the X-33. The Shuttle serves as an ideal target to provide data for development of measurement and processing techniques since there is a vast aeroheating data base that currently exists, particularly on boundary layer transition. In addition, Shuttle aeroheating flight data is collected during each reentry using surface thermocouples.

STS-96 Data Acquisition

Infrared imagery was collected during the STS-96 landing at Kennedy Space Center, Florida, on June 6, 1999. Figure 5 shows the ground track of the STS-96 as it approaches over Cuba, over South Florida to the landing strip at KSC. The insert shows the segment of the ground track where infrared data were acquired and the location of the BMDO/ISTEF tracking site. Image data were acquired just prior to the heading alignment circle when the astronauts take control of the approach and landing of the vehicle. For this flight, the Orbiter entered on orbit number 153, which is earlier than nominal. Data were acquired directly South of the site after a sky search. Upon initial image acquisition, the automatic tracking system successfully tracked the Orbiter until it flew almost directly over the site and the telescope gimbals were not able to keep up with the Shuttle's motion across the sky. For Shuttle, unlike X-33, optimal placing of ground-based camera systems is difficult due to deorbit "go/nogo" options exercised only minutes prior to deorbit, which can significantly change the ground track.
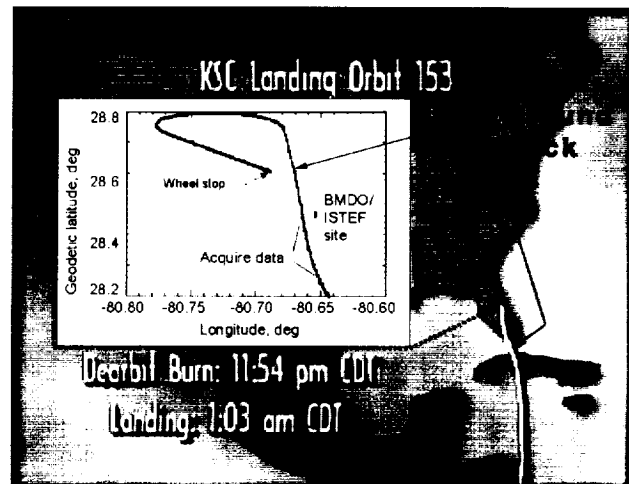

Fig. 5 STS-96 landing approach ground track with data acquisition segment.

Figure 6 shows the Orbiter's Mach number and the corresponding altitude as it approached the landing runway at KSC. These graphs are generated from the post-flight trajectory provided by the Orbiter Project Office at JSC. Also, shown on the graphs is the segment of infrared image acquisition. As seen, the initial data acquisition altitude is about 70,000 ft; however, the slant range was about 101,000 ft with the elevation angle about 46° above the horizon. When the Orbiter flew over the site the altitude was about 60,000 ft, which closely corresponds to the slant range. During acquisition, the Mach number varied from about 1.95, soon after the pressure probe deployed which acquires data for onboard Mach number calculations, down to about 1.48. At these conditions, the windward surface of the

4

Orbiter residual heat from the earlier high-heating reentry phase was sufficient for infrared measurements.
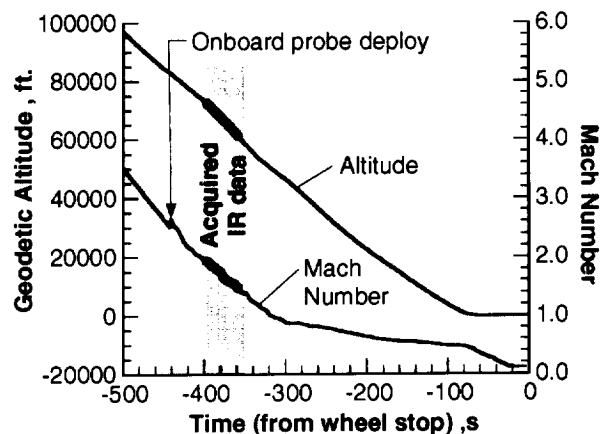

Fig. 6 STS-96 geodetic altitude and Mach number near landing at KSC.

Fig. 7 STS-96 body axis orientation near landing at KSC.

The orientation of the Orbiter as it approaches landing at KSC is given in Fig. 7. These graphs were generated from post-flight trajectory data obtained from the Orbiter Project Office at JSC. During infrared imaging, labeled "Acquire data" on the graph, the side-slip angle is nearly constant at about $-1.0°$, while the angle of attack and roll angles both start out at about $10°$, with the roll angle approaching $0°$ and the angle-of-attack reducing slightly by the end of the data acquisition.
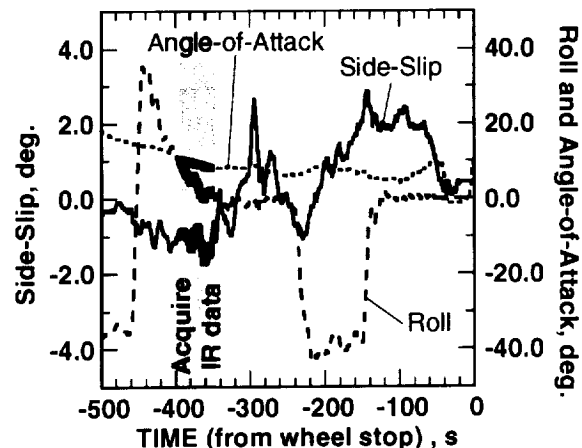
STS-96 Thermocouple Data

On each Orbiter reentry, limited thermocouple data is collected for purposes of diagnostics after the flight. Figure 8 presents the windward surface thermocouple flight data acquired during the STS-96 reentry. The reference time on each graph is from entry interface (400,000 ft) and the locations of the thermocouples on the bottom surface of the Orbiter are shown. The three digits on each figure represent the last three digits of the measurement system identification (MSID), JSC flight
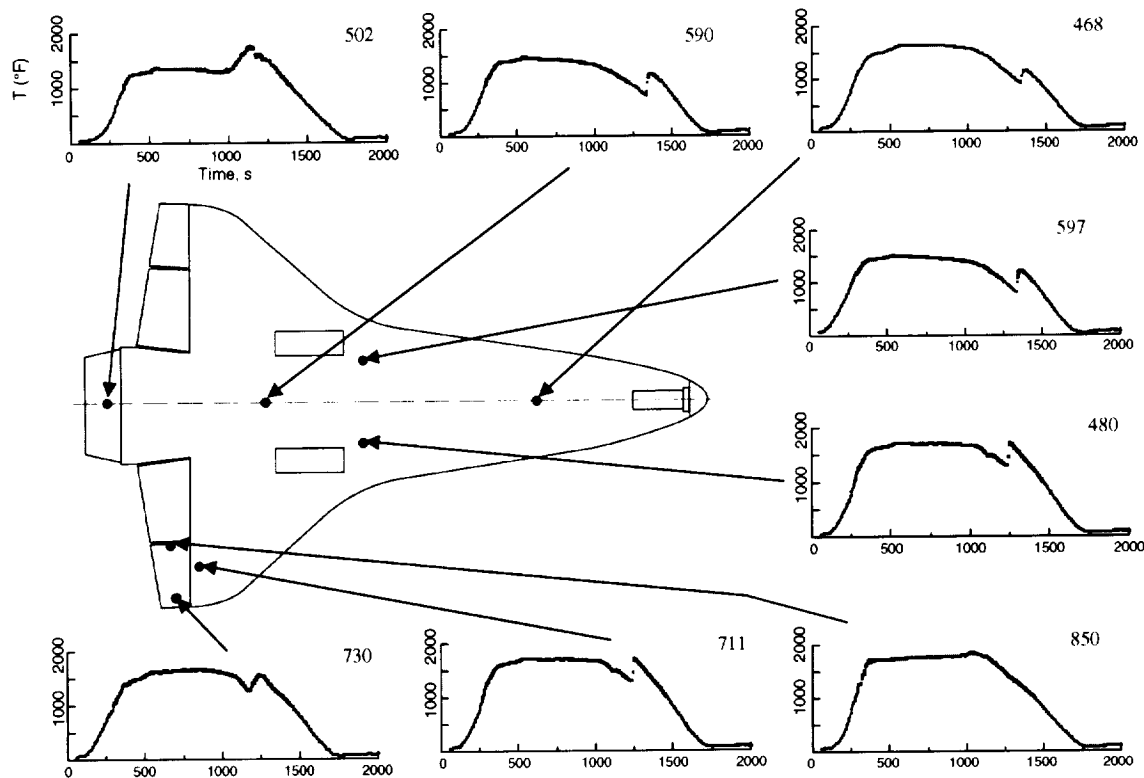

Fig. 8 STS-96 windward thermocouple data from entry interface (400,000 ft) to landing.

5

data identification nomenclature. The graphs show the temperature rise during boundary layer transition from laminar to turbulent. The rise in temperature is relatively quick, on the order of 10's of seconds. Also, noting the times of the temperature pulse peak, it is observed that transition occurs first near the rear of the body (on the body flap) and moves forward on the Shuttle Orbiter with time.

The thermocouple data corresponding to the time interval when the infrared data were acquired are given in Fig. 9. Shown are the centerline thermocouple measurements which, when the infrared data were acquired, ranged between about 325 to 175 °F (436 to 353 K).
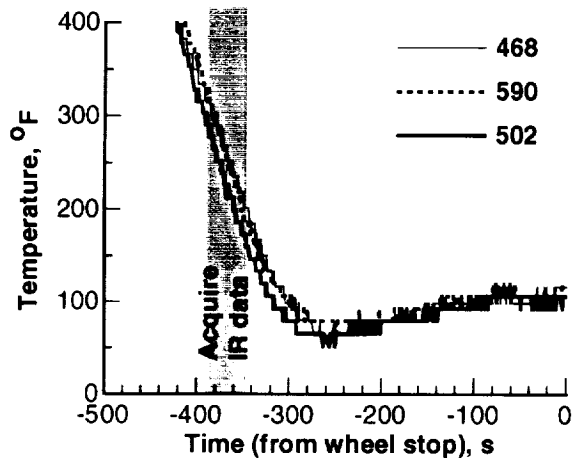

Fig. 9 STS-96 centerline windward thermocouple data(expanded scale).

STS-96 Infrared Radiance Data

Two sets of midwave (3-5 μm) infrared data were collected during STS-96 reentry, one using the 24" aperture telescope and a separate set of data using the 12.5" aperture telescope. Over 1260 images from each sensor were collected. Attempts were made to acquire images using the long-wave infrared (LWIR) detector (8-12 μm), but a malfunction of the accompanying controller prevented its use. Also, the 12-bit digital system encountered problems so that the data collected was confined to 8-bit analog. Figure 10 shows a typical infrared image taken early in the data acquisition time period. The bright areas in the image correspond to "hotter" surfaces when compared to darker areas (assuming constant surface emissivity). For the image shown, this is approximately true since the emissivity of the reinforced carbon/carbon (RCC) wing leading edges (and nose cap) and the reacting cured glass (RCG, "black glass") tiles over most of the windward surface are nearly equal for the temperatures of the Orbiter during this time. The detector settings were optimized for the bottom surface of the Orbiter (i.e. maximum temperature resolution) with the consequence that the RCC leading edges were in saturation for the measurements. The extra bright wing leading edge and the nose cap in the figure are in detector saturation, which for the set-

ting used for this image corresponds to temperatures in excess of 560 K (548 °F). [The other detector setting used during the flight saturated at about 700 K (800 °F).] The temperatures deduced from this and subsequent radiance infrared image show the leading edge as warm areas (as expected) and a fairly benign (approximately uniform) windward heating. The transformation of the radiance images to temperature is discussed next.
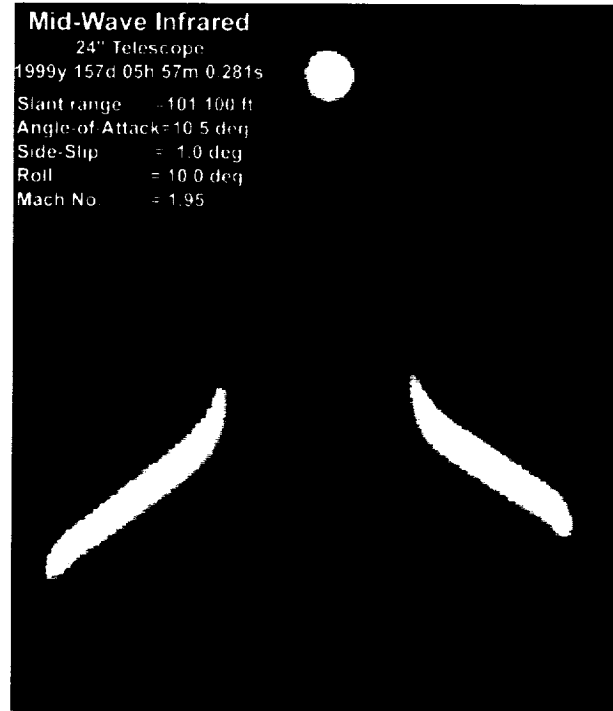

Fig. 10 Infrared image of STS-96 during reentry.

STS-96 Infrared Temperature Data

The transformation of the radiance infrared data to surface temperature depends on several factors, including vehicle surface emissivity, path transmittance, atmospheric radiance, optics radiance, and other calibration factors from a "bench" and "field" calibration obtained during setup of the telescope/detector system prior to flight.

The method used to obtain the surface temperature is to develop a lookup table of the detector response (in count units) as a function of surface temperature using the following equation:

$$R = G_{set}L_p(T) + B_{set} \qquad (1)$$

where,

$$L_p(T) = L_{BB}(T)\varepsilon(T)\tau_{atm} + L_{path}$$

The surface emissivity of the Orbiter has been obtained from NASA-Ames Research Center and is shown in Fig. 11 (data contained in database, http://asm.arc.nasa.gov, TPSX WEB V2, "Thermal Protection System Expert and Materials Properties"). For the calculations of temperature, the RCG emissivity

values were used since the RCC surface was in saturation. Note, however, that at the surface temperatures of the images (on the order of 400 K) that the emissivity differs by only about 10%. It is also assumed for this analysis that the surface emissivity has no wavelength dependence
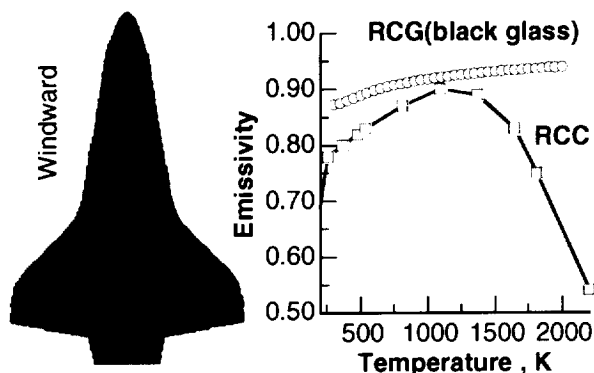

Fig. 11 Orbiter windward surface emissivity as a function of temperature. (from NASA-Ames Research Center)

The atmospheric path transmittance (τ_{atm}) and the atmospheric radiance (L_{path}) have been calculated using the atmosphere model program, MODTRAN[7]. Local meteorology soundings and measurements obtained from Patrick AFB during the time of STS-96 reentry were used as inputs to the program to obtain as realistic estimates as possible. Two other verification checks were performed on the MODTRAN output. These are the "sky background" (i.e. a measurement of the background sky at various telescope elevations without the target), and by using a calibrated stellar source, Alpha Bootis[8]. Both input sources were within expected radiance errors for each setup. The resulting MODTRAN data used in the extraction of temperature is given in Figs. 12(a) and 12(b) which shows the path transmittance and the atmospheric radiance as a function of time from STS-96 wheel stop. The time interval shown includes the interval in which the infrared data were acquired.

Two calibrations are performed and used to interpret the flight infrared images, a "bench calibration" and a "field calibration". The bench calibration establishes the initial relationship between the irradiance and the sensor output. This is accomplished in the lab with a calibrated blackbody source. A temperature is selected for the blackbody and the sensor output is analyzed for average intensity and standard deviation. By repeating this procedure for various temperatures over the dynamic range for the selected setup, an incidence radiance and sensor output relationship can be found in the form of a linear equation. The other calibration is the field calibration, which consists of placing a calibrated blackbody source

beyond the minimum distance the telescope can focus in the field. This calibrates the system as a whole, including the optics. Using several interim setup procedures results in a complete transfer function that combines the effects of the sensor, the optics (including filters), and the recording device(s). The calibration curve resulting from these calibrations for "setup 2", the 24" aperture telescope, and the mid-wave infrared (MWIR), (3-5 μm) detector is given in Fig. 13. The system output (counts) can be transformed to "apparent" radiance of the vehicle by application of this curve ("apparent" here means the effects of the atmosphere have not been fully taken into account). Included on the graph are error bar estimates at each of the calibration points. This is one of two calibration curves used in the STS-96 data reduction and interpretation process.
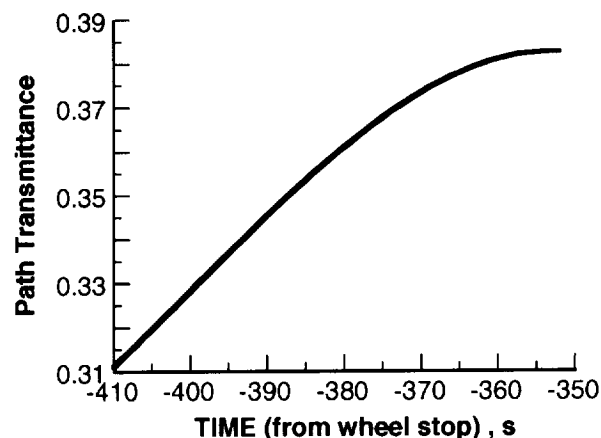
(a) Path Transmittance
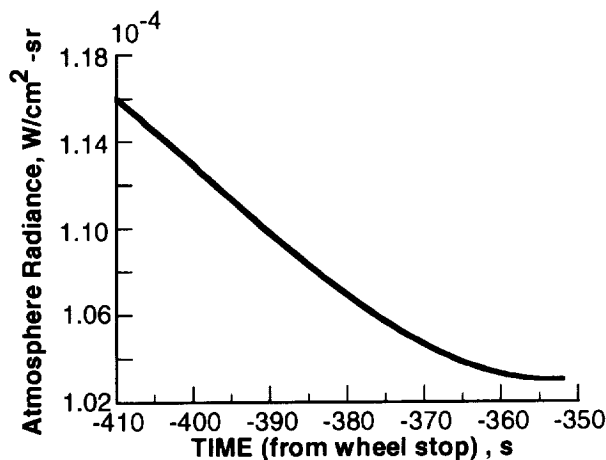
(b) Atmosphere Radiance

Fig. 12 Atmosphere path transmittance and radiance during STS-96 infrared data acquisition using MODTRAN.
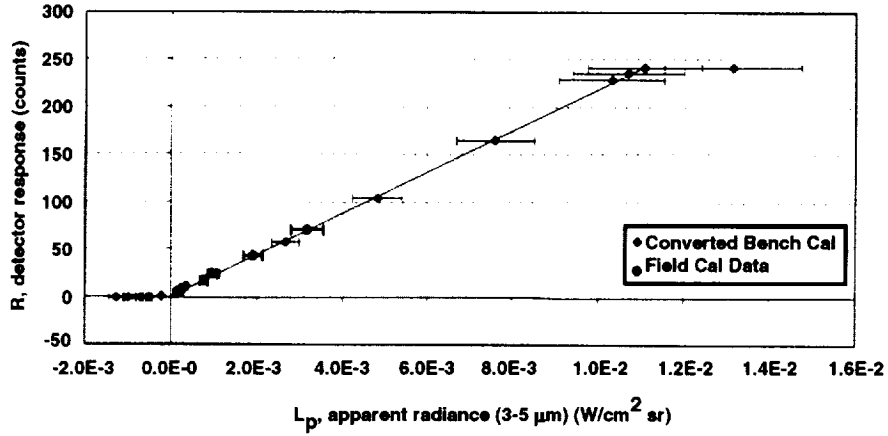
7

Fig. 13 BMDO/ISTEF 24" telescope, MWIR detector, system response (for setup 2)

Applying the elements previously discussed to the 1200[+] frames of radiance data collected on STS-96 results in a corresponding global temperature. A typical example of one of the frames is given in Fig. 14 which shows the surface temperature (K) as a spectrum of colors ranging from blue (cool) to red (hot), as noted on the side of the image. The results are preliminary in nature in that directional surface emissivity and possibly low resolution effects have not been accounted for (resulting in the apparent drop in temperature around the wing leading edges.

Uncertainty Estimates

The errors associated with the radiance measurements contain several elements and are setup dependent. Table 1 provides the error sources as well as estimates of their contribution to the overall uncertainty. The radi-

ance errors shown are considered worst case and are not uniform over the measurement range as can be observed, for instance, from the error bars in Fig. 13. To obtain a corresponding approximate error in the temperature, consider the relative error relationship between temperature and radiance, namely:

$$\frac{\delta T}{T} = \frac{\left(e^{\frac{C_2}{T}} - 1 \right) T}{e^{\frac{C_2}{T}} C_2} \left(\frac{\delta L_m}{L_m} \right) \tag{2}$$

where,

$$C_2 = \frac{hc}{\lambda k} \tag{3}$$

For the temperatures encountered during STS-96 and the measurement wavelengths, the estimate of tem-

Fig. 14 STS-96 global temperature data from ground calibrated infrared observations.

8

Table 1. Error estimate for BMDO/ISTEF MWIR 24" Imaging System

ERROR SOURCES	For Setup 1	For Setup 2
Atmosphere self radiance and attenuation	5.0%	5.0%
Blackbody uncertainty (Includes emissivity, temperature, and uniformity uncertainty)	2.5%	2.5%
System Noise Estimate (Derived from standard deviation of uniform source under observation- worst case)	7.1%	10.2%
Least Square linear error estimate (Mean difference of known source data points)	14.0%	3.4%
RSS ERROR	16.7%	12.1%

perature error for the radiance errors shown above is less than 2%, which shows that a large uncertainty in radiance does not necessarily produce a large error in temperature.

Thermocouple and Infrared Temperature Comparisons

A four-step image reconstruction methodology, for associating infrared image pixels with thermocouple locations, was developed using image processing and simplified photogrammetry theory.[9] The approach has been made general enough to allow for automated processing of the large number of images acquired in this study. First, for a given frame, a projection of the 3-D Orbiter geometry[10] on the detector image plane is created based upon post-flight vehicle attitude data (Fig. 7) and the attitude of the telescope. Next, the Orbiter-geometry projection is scaled based upon the known characteristics of the imaging system. From there, the edges of the Orbiter in the IR image frame are detected. This step was made difficult by the slightly blurred edges associated with image resolution, reduced signal due to possible drop-off of directional emissivity, and low signal on the Orbiter body flap as compared to background signal from the sky. To handle this a gradient/thresholding process was used. Finally, the Orbiter-geometry projection is registered with the measured IR image by enclosing the edges of the two images in a rectangle and overlaying one on top of the other. The details of the complete process are given in Reference 9. An example of the final result is given in Figure 15, which shows the location of the eight thermocouples on the measured image. [Note: the size of the dots representing the thermocouples is enlarged for display purposes.]

Once the pixel locations of the thermocouples have been identified, the difference between the thermocouple and infrared temperatures can be calculated for each frame. The temperature differences do not necessarily provide an absolute temperature measure, because of flight thermocouple measurement uncer-

tainties. Uncertainty estimates based upon previous thermocouple Orbiter thermocouple sensor measurements[11] are about 1 to 2%, resulting in an inferred surface temperature of about 5-10%. Thus, the question is, can an independent calibrated temperature global infrared image (without thermocouples) provide as good as flight temperature data as thermocouples?
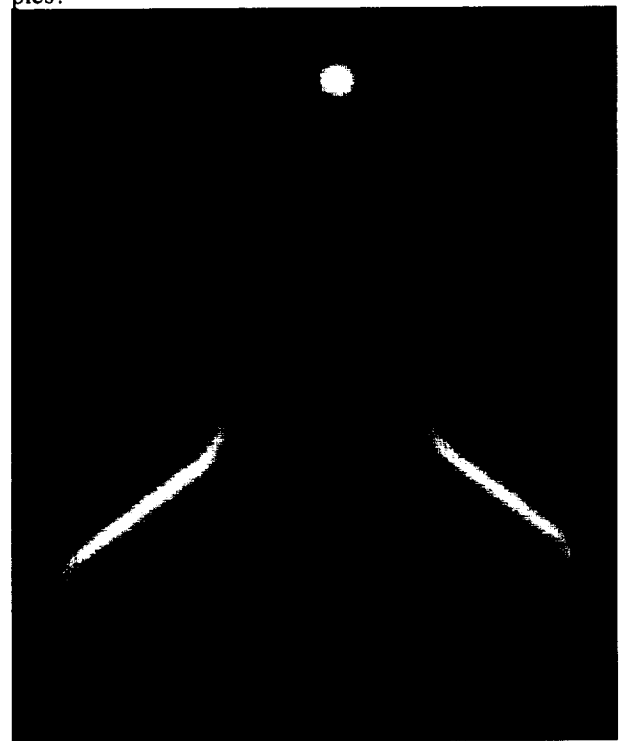

Fig. 15 Location of thermocouples on infrared image.

Figure 16 shows the relative difference between the flight thermocouple temperatures and the ground calibrated infrared temperatures. All temperature differences are less than about 5%, except for the thermocouple measurement near the elevon gap (number 850), that clearly shows a bias. A possible explanation for this bias is that the infrared resolution ranges from about 3 to 6 inches at the image distances and the thermocouple measure at a point (essentially). Thus, with a sharp temperature gradient, as would
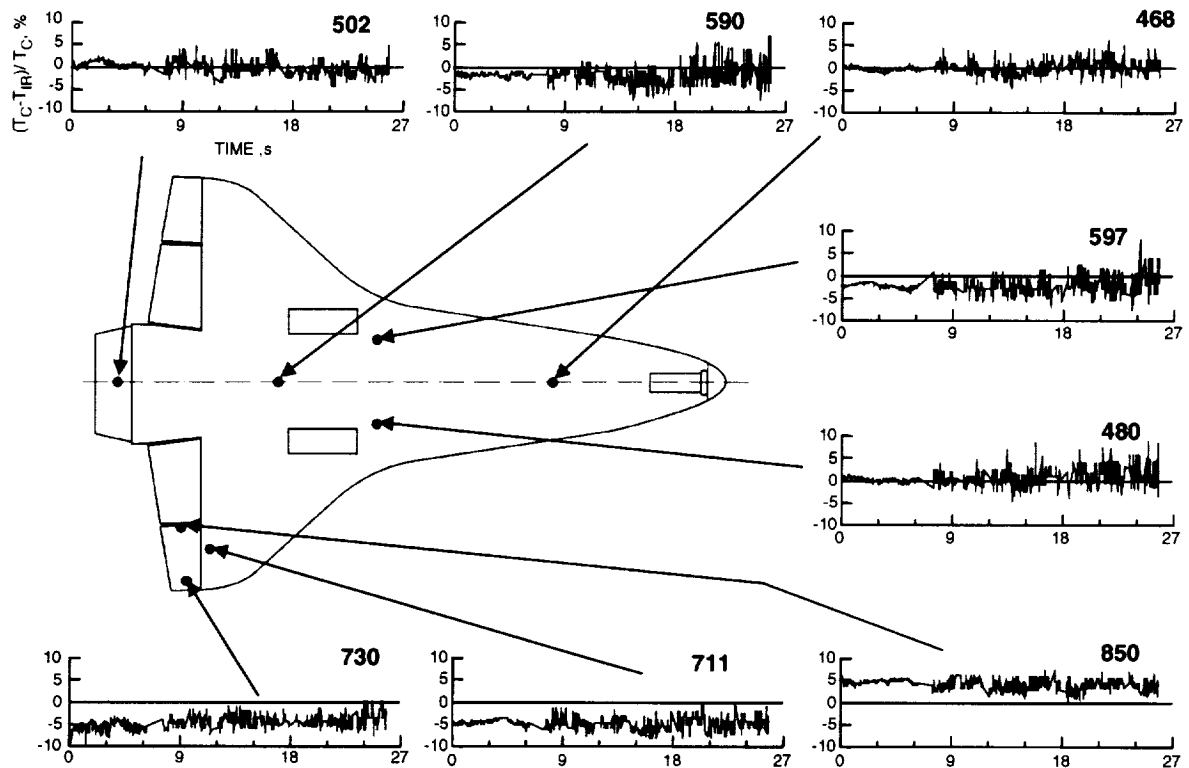
9

Fig. 16 Thermocouples and infrared temperature differences for STS-96.

exist at, or near, the elevon gap, the infrared temperatures would tend to average to a different value. In general, however, the differences are less than about 5%, which lends credence that an independent calibrated global infrared image (without thermocouples) can provide comparable flight temperature data. However, when thermocouple data is available, the preference would be to integrate this data into the data processing of the infrared images to take full advantage of the thermocouple measurements. In general, thermocouple data can be used as a calibration source (see ref.. 9), or a validity check on the calibration and processing technique. The later is what has been done in this report.

Summary

An infrared experiment is being developed as a general versatile tool to provide quantitative flight global heating data for reentry vehicles at hypervelocity speeds. The experiment is called the Infrared Sensing Aeroheating Flight Experiment (ISAFE) and its primary goal is to identify, monitor, and quantify hypersonic boundary layer transition for the X-33 vehicle during flight. This includes, specifically, the global mapping of the transition movement over the windward surface. The data collected during flight will serve as a calibration and validation of current boundary layer transition prediction techniques. In addition, the flight experiment goal is to provide benchmark laminar, transitional and fully turbulent global aeroheating data in order to validate existing wind tunnel and computational results, and to advance aeroheating technology.

The Shuttle Orbiter flights were selected as targets of opportunity to demonstrate the capability of the ground-based infrared equipment and the data reduction techniques, in order to mitigate the aeroheating experiment risks prior to the first flight of the X-33. The Shuttle serves as an ideal target to provide data for development of heating measurements and processing techniques since there is a vast aeroheating database that currently exists. Also, Shuttle aeroheating flight data is collected during each reentry using surface thermocouples.

Infrared imagery was collected during the STS-96 landing at Kennedy Space Center, Florida, on June 6, 1999. The calibrated radiance infrared images were transformed to surface temperatures using a combination of ground calibrations and meteorology measurements taken at the time of the mission. Several image-processing techniques were developed and applied to the infrared images to find the thermocouple locations in the image in order to generate temperature differences. The differences between flight thermocouple and infrared temperature data were generally less than about 5%, which is comparable to the expected accuracy of both types of aeroheating measurements. Thus, it has been shown that an inde-

10

pendent calibrated temperature global infrared image (without thermocouples) provide flight temperature data comparable in accuracy to thermocouples.

Major accomplishments have been made with the data from the Shuttle mission infrared measurements paving the way for a high probability of success for application to the X-33 flights. The work to date on the Shuttle mission demonstrates the feasibility of applying the ground-based infrared measurements and data reduction to the X-33 vehicle during peak heating and boundary-layer transition portion of the flight trajectory.

Acknowledgments

References

1. Berry, S. A.; Horvath, T. J.; Hollis, B. R.; Thompson, R. A.; and Hamilton, H. H.: "X-33 Hypersonic Boundary Layer Transition," AIAA Paper 99-3560, June 1999.

2. Bouslog, S. A.; An, M. Y.; and Derry, S. M.: "Orbiter Windward-Surface Boundary-Layer Transition Flight Data," NASA CP3248 Part 2, Edited by D. A. Throckmorton, NASA-Langley Research Center, April 1995.

3. Bertin, J. J., Hayden, T. E., and Goodrich, W. D.: "Shuttle Boundary-Layer transition Due to Distributed Roughness and Surface Cooling," *Journal of Spacecraft and Rockets*, Vol. 19, No. 5, Sept.-Oct., 1982, pp 389-396

4. Thompson, R. A.; Hamilton, H. H.; Berry, S. A.; and Horvath, T.J.: "Hypersonic Boundary Layer Transition for X-33 Phase II Vehicle," AIAA Paper 98-0867, January 1998.

5. Horvath, T. J.; Berry, S. A.; Hollis, B. R.; Liechty, D. S.; Hamilton, H. H.; and Merski, N. R.: "X-33 Experimental Aeroheating at Mach 6 Using Phosphor Thermography," AIAA Paper 99-3558, June 1999.

6. Hollis, B. R.; Horvath, T. J.; Berry, S. A.; Hamilton, H. H.; and Alter, S. J.: "X-33 Computational Aeroheating Predictions and Comparisons with Experimental Data," AIAA Paper 99-3559, June 1999.

7. Acharya, P.K., Robertson, D.C. and Berk, A. "Upgraded Line-of-Sight Geometry Package and Band Model Parameters for MODTRAN," Phillips Laboratory Technical Report PL-TR-93-2127, Geophysics Directorate, Hanscom AFB, MA, 1993.

8. Engelke, C. W.,"LWIR Stellar Calibration: Infrared Spectral Curves for 30 Standard Stars," Technical report 908 Appendix B, MIT/Lincoln Labs, Lexington, MA, Apr. 10, 1991

9. Bozung, T.J.: "Space Shuttle Infrared Image Calibration using Thermocouple Data," GWU Master's Thesis, to be published March, 2001.

10. Weilmuenster, J. K.; Gnoffo, P. A.; and Greene, F. A.: "Navier-Stokes Simulations of Orbiter Aerodynamic Characteristics," NASA CP3248 Part 1, Edited by D. A. Throckmorton, NASA-Langley Research Center, April 1995.

11. Hartung, L. C. and Throckmorton, D. A., "Space Shuttle Entry Heating Data Book," Vol. I-STS-2, NASA RP 1191 Part 1, May, 1988.